



ارائه شده توسط:

سایت ترجمه فا

مرجع جدیدترین مقالات ترجمه شده

از نشریات معتبر



# Behavior of closely spaced double-pile-supported jacket foundations for offshore wind energy converters



Cihan Taylan Akdag\*

Torbali Vocational School of Higher Education, Geotechnics Program, Dokuz Eylül University, 35860 İzmir, Turkey

## ARTICLE INFO

### Article history:

Received 28 September 2015

Received in revised form 30 January 2016

Accepted 17 April 2016

### Keywords:

Offshore wind energy converters

Closely spaced piles

Jacket foundation

Numerical simulation

Combined loading

Load distribution

## ABSTRACT

As the offshore wind energy production units move to deeper waters the design of their foundations demand more creative and complex approaches especially for large turbines (i.e. ~5–7 MW). In this article, a novel piled foundation alternative with closely spaced double piles at the edges of the jacket is studied for various pile spacing and lengths. A numerical parametric study was carried out to understand the effects of pile spacing and pile length on the behavior of the novel supporting system under monotonic combined loading in very dense sand. Prior to the analysis, the numerical model is validated in field tests with single-pile and double-pile configurations. The contribution of closely spaced double piles to the overall foundation response and load distribution among the piles were investigated. The response of the foundation was evaluated considering the horizontal load-head displacement, moment-head rotation, and initial stiffness of the soil-pile system. It is found that the response of the recommended foundation system is superior to that of a rather conventional system with single piles at the edges. The results indicate that the piles on the tension loading side evidently carried lower loads than those on the compression side. Moreover, the disposition of the piles is more important on the tension side, as the trailing piles carried considerably lower loads than the leading piles. It is found that the double pile system with a pile embedment length  $L/2$  and a pile spacing of  $S = 5D, 6D$  provides better response, where  $L$  is the embedded pile length of conventional system and  $D$  is the diameter of pile.

© 2016 Elsevier Ltd. All rights reserved.

## 1. Introduction

The importance of renewable energy is significantly increasing, and the utilization of offshore wind energy has been growing. Within the next few decades, a vast number of offshore wind energy converters (OWECs) shall be erected to supply a large portion of our energy needs [1]. It is stated in the report of European Wind Energy Association [2] that the next step for wind energy is offshore wind farms in deep waters, and projects of deep OWECs are being developed in Europe. In this respect, selecting and designing an appropriate OWEC foundation type is an essential challenge for geotechnical engineers, as the foundation is the critical part of the design of OWECs. Therefore, the design of OWEC foundations has been the focus of several studies [3–5]. Gravity, monopile, and monopod suction bucket foundations are suitable for shallow and moderate water depths up to 25 m. Conversely, there is a need to enhance existing foundation systems for large wind turbines in deep waters (deeper than 30 m). Thus, innovative

substructure concepts regarding multi-footing configurations have recently been under research and development [6,7]. Kim et al. [6] performed a parametric study to understand the group effect of tripod bucket foundations on the bearing capacity. The behavior of a three-bucket jacket substructure under long-term cyclic loading was investigated by Lupea et al. [7]. Shi et al. [8] stated that the jacket foundation is becoming progressively more interesting and is a good option for water depths between 30 and 80 m. Achmus et al. [9] indicated that for larger water depths, tripod and jacket foundations are more appropriate. However, the combined horizontal and vertical loading applied to individual piles of tripod and jacket foundations significantly increase with the water depth. In this regard, the foundation of wind turbines should ensure an adequate bearing capacity against such loading conditions in deep waters. Consequently, this study is focused on a novel supporting system of the jacket foundation for OWECs in deep waters. The conventional jacket foundation is supported by four piles positioned at the edges of the construction (Fig. 1a). For the recommended innovative foundation, the available jacket foundation system was supported using closely spaced double piles for each edge (Fig. 1b). To keep the symmetry of the foundation system on both the x- and y-axes, each leg was designed with closely spaced double piles

\* Corresponding author.

E-mail addresses: [taylan.akdag@deu.edu.tr](mailto:taylan.akdag@deu.edu.tr), [akdagcih@b-tu.de](mailto:akdagcih@b-tu.de)

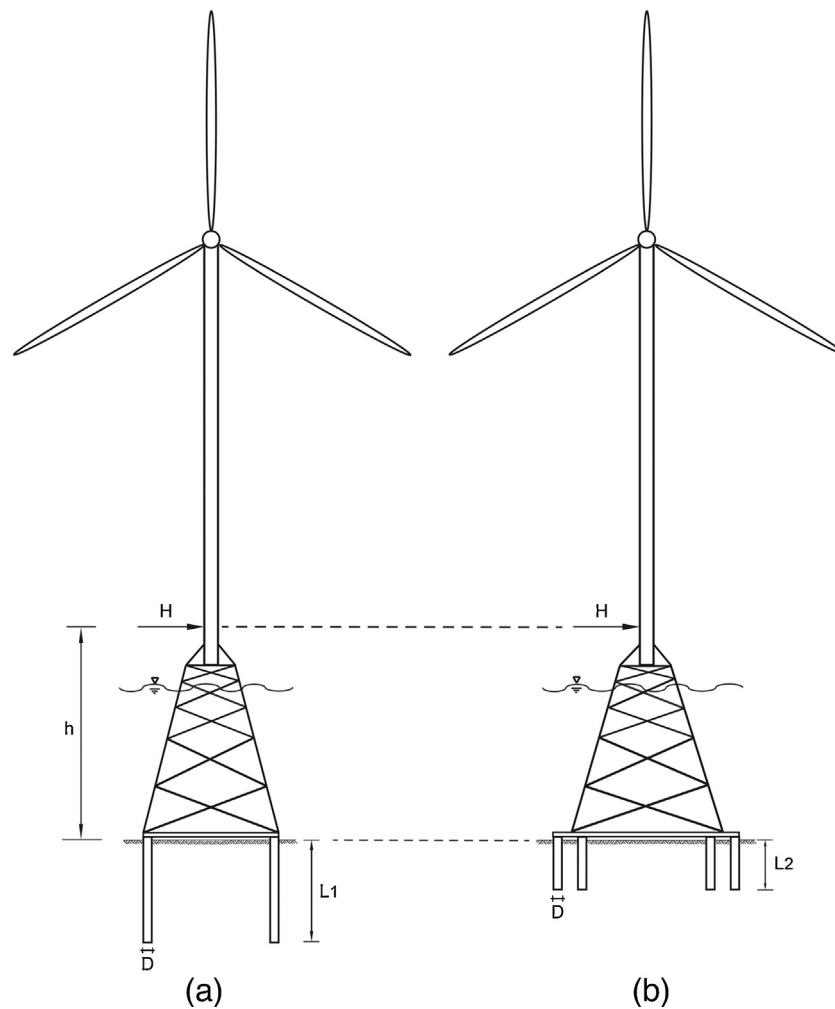


**Fig 1.** Schematic sketch of OWEC on foundation systems: (a) conventional pile-supported jacket ( $L1 = 12.5D$ ); (b) jacket with closely spaced double piles ( $L2 = 6.25D$ ,  $S = 3D$ ).

arranged diagonally. In some cases, the depth profile of the seabed shows that chalky soil layers can exist beneath the sand/clay layers, i.e., in the Baltic Sea north of Rügen, large chalk deposits are found beneath the glacial till [12]. It is noted in the study of Dührkopf and Barbosa [13] that the pile destroys the chalk during installation, and it is estimated that the destroyed chalk around the pile characterizes the response of the foundation system under cyclic loading. The results of a cyclic test on chalk obtained from the Wikinger Site show an obvious decrease in the shear stress during cycling [13], which demonstrates the dilative nature of chalk when sheared. In this respect, the recommended relatively short closely spaced piles promise a fine solution to avoid installing the piles into chalky soil.

Moments arising from wind and wave loading are transferred to vertical loads on the individual piles. Thereby, the individual piles of the jacket foundations are exposed to horizontal and vertical combined loading, that is, combined tension and compression loading. The effects of combined loading on the behavior of piles are scarce in the literature, especially for offshore structures, and have not been studied yet for closely spaced piles. The study of Achmus and Thieken [10] regarding monopile behavior under combined horizontal and vertical loading indicates that combined compression loading leads to favorable and combined tension loading mostly unfavorable influences on the system stiffness. Akdag and Özden [11] found that a vertical load significantly improved the performance of the reinforced concrete (RC) and RC-with steel fiber piles, according to lateral loading and lateral + axial loading model pile test results.

Although there have been several experimental and numerical based studies on the behavior of closely spaced piles [14–16], the response of closely spaced piles for an OWEC foundation has not been studied yet. It is well known that the efficiency of the pile is considerably affected when the piles are installed close to each other due to overlapping soil reaction zones. McVay et al. [14] found that the group efficiency at pile spacing ( $S$ ) of  $3D$  was 22% less than the group efficiency at a spacing of  $5D$  according to centrifuge tests conducted on the closely spaced piles, where  $D$  and  $S$  are the pile diameter and the center-to-center distance between the piles, respectively. The influence of the pile spacing and the number of piles on the behavior of closely spaced piles was investigated using the finite element method [15]. The behavior of the piles in the group was compared with the behavior of a single pile, and the variation of the displacement amplification factor was quantified. It was determined that the displacement amplification factor depends on the horizontal load level, and the factor attains its maximum value at the initial load level [15]. Model pile tests were performed in various closely spaced pile layouts by Kim and Yoon [16]. It was emphasized that group interaction effects in closely spaced piles reduce the load-carrying capacity for all rows (i.e., trailing row, middle row, and leading row) relative to the single pile response. It was also observed from the tests that the soil reaction strongly depends on the closely spaced pile layout and pile spacing. It was remarked that load reduction factors to compute the load carried by each pile depend on the pile position in closely spaced piles [17]. Brown et al. [18] found that the piles in the leading row supported

a large proportion of the total load and responded similarly to a single pile according to field tests on a group of piles.

Behavior of piled jacket foundations of OWECs is a rather complex phenomenon comprising the structural and geotechnical design aspects. One may notice that particularly fatigue behavior of the jacket portion has been studied under aerodynamic and hydrodynamic loading conditions [19,20]. In such studies researchers did not pay attention to the nonlinear soil-pile interaction. For instance, Alati et al. [19] just assumed linear soil response giving emphasis to the structural behavior. In this study, however, nonlinear pile-soil-pile interaction and overlapping of heavily stress soil zones around laterally displacing piles are taken into consideration.

A numerical-based parametric study was conducted to understand the effect of pile spacing and pile length on the behavior of a jacket foundation supported by closely spaced double piles in very dense sand. The results such as the load-head displacement, the moment-head rotation, and the initial stiffness of the foundation system are assessed. Ultimate load capacity of the reference foundation systems was determined. The soil reaction along the individual pile length is determined, and the influence of the pile spacing and pile length on the load distribution is presented. The effect of the combined compression and tension loading on the load distribution among the piles is evaluated in this study.

## 2. Numerical model

A three-dimensional finite element (FE) model of a conventional pile-supported jacket and a jacket supported with a closely spaced double-pile foundation system was developed and utilized in the scope of a parametric study for large (5–7 MW) offshore wind turbines. This numerical-based study was implemented using the finite element program PLAXIS 3D [21]. Preliminary analyses were performed for the determination of mesh fineness and model dimensions for the purpose of achieving an adequate accuracy of the results and avoid the influence of boundary condition. Consequently, the depth of the soil under the pile was left five times the pile diameter ( $5D$ ), and the soil was extended  $13D$  in the  $x$ - and  $y$ -directions around the supporting system. An exemplary mesh of the finite element model for closely spaced double piles configuration is presented in Fig. 2. The finite element model plan view of the single-pile configuration and the plan view and cross-section of the closely spaced double-pile configuration along with the geometrical properties and loading method are shown in Fig. 3. It should be noted in Fig. 3 that the soil was divided into volumes in order to obtain a finer mesh around the piles. The volumes around the piles were defined by surfaces located within an area of  $5D \times 5D$  around each pile for the single-pile configuration. The distance of the defined volume surfaces was set to  $2D$  in the  $x$ - and  $y$ -directions from the pile surface around each leg of the double-pile configuration, as seen in Fig. 3a and b.

The hardening soil model with a small strain stiffness (HSsmall) according to Benz [22] was utilized for the simulation of very dense sand in this study. It is stated in the current studies that the HSsmall model is an advanced constitutive soil model and that prediction of the behavior is more accurate under small strain [23,24]. The HSsmall model can be determined as an extension of the Hardening Soil (HS) model. In contrast to an elastic perfectly plastic model, the HS model utilizes an elasto-plastic behavior and takes into account the stress-dependent stiffness of the soil. In addition to all features of the HS model, the HSsmall model considers the very small strain and its non-linear dependency on the strain amplitude. Therefore, it was decided to use the HSsmall soil model in the scope of this study.

Before the parametric study, the numerical model was validated by comparison with the field test results presented in detail in

**Table 1**

Very dense sand parameters considered for the back-calculation of the Mustang Island field test and a parametric study.

Parameter	Sand
Buoyant unit weight, $\gamma'$	10.37 kN/m <sup>3</sup>
Poisson's ratio, $\nu$	0.20 [-]
Power for stress level dependency of stiffness, $m$	0.50
Internal friction angle, $j'$	39.0°
Dilation angle, $y$	9.0°
Cohesion, $c'$	0.1 kN/m <sup>2</sup>
Initial void ratio, $e_{init}$	0.4[-]
Secant stiffness in the standard drained triaxial test, $E_{50}^{ref}$	$8.0 \times 10^4$ kN/m <sup>2</sup>
Tangent stiffness for primary oedometer loading, $E_{oed}^{ref}$	$5.3 \times 10^4$ kN/m <sup>2</sup>
Unloading/reloading stiffness at engineering strains, $E_{ur}^{ref}$	$2.4 \times 10^5$ kN/m <sup>2</sup>
Reference shear modulus at very small strains, $G_o^{ref}$	$1.55 \times 10^5$ kN/m <sup>2</sup>
Shear strain at which, $G_s = 0.722G_o, \gamma_{0.7}$	$0.1 \times 10^{-3}$ [-]
Failure ratio, $R_f$	0.90 [-]
Interface, $R_{inter}$	0.67[-]

Section 3. The “Mustang Island” field test was performed in very dense sand conditions, and it was stated that the water table was maintained above the ground surface during lateral loading to simulate offshore conditions [25]. Considering the features of the test, the very dense sand properties that were used for the validation of the numerical model were also used in the simulation of parametric study. The soil parameters for very dense sand used in the model are presented in Table 1.

The piles were modeled using open tubular steel piles made of structural plate elements. The planar plate elements are 6-node triangular elements based on the theory of plates with transverse shear deformations included. The plate deflects due to shear forces and bending moments according to this theory. Besides, elongation of the plate as a result of axial force is taken into consideration. In the modeling of the pile, a diameter  $D=2m$ , a wall thickness of  $t_{pile} = 0.05m$  and various lengths were considered. The modulus of elasticity  $E = 210GPa$ , the Poisson's ratio  $\nu = 0.2$ , and the buoyant unit weight  $\gamma' = 68kN/m^3$  were set for the pile material properties. The pile head is extended  $0.5D$  above the soil surface. The jacket structure over the piles was assumed to be quite rigid and was modeled with an almost stiff upper plate. The upper plate was combined at the pile head with a very large modulus of elasticity  $E = 1 \times 10^{10}GPa$ , considering that the connection between the pile head and jacket structure is constructed quite stiff. The thickness of the upper plate was set to  $t_{plate} = 0.05m$ , and the unit weight of plate was adjusted to provide a constant plate weight ( $1MN$ ) for each model.

Analyses were performed under combined vertical ( $V$ ), horizontal ( $H$ ), and moment ( $M$ ) actions for monotonic loading conditions. The loads acting on the foundation system were represented in the numerical model in such a manner that the moment ( $M$ ) arising due to the distance of the horizontal load to the upper plate ( $h$ ) (Fig. 1) was represented by lateral load ( $H$ ) and moment ( $M = H \cdot h$ ) by defining a pair of vertical loads in opposite directions and dead load ( $V$ ) at the upper plate level as shown in Fig. 3b. A typical vertical load for large offshore wind energy converters was applied to the center of the upper plate. The modeled upper plate weight on the piles was also considered while applying the vertical load  $V = 10MN$  to simulate the total weight of wind turbine above the supporting system. A constant distance of the horizontal load to the upper plate  $h = 50m$  was set in the scope of this study. The horizontal load  $H = 8MN$  was applied in the  $x$ -direction to the center of the plate in the parametric study.

Numerical analyses were conducted in several calculation steps. In the first step, the geostatic stresses in the model consisting of soil elements only were calculated by the application of gravity loading. In this step, a coefficient of earth pressure at rest,  $k_0 = 1 - \sin\phi'$ , was utilized. Subsequently, the predefined steel elements

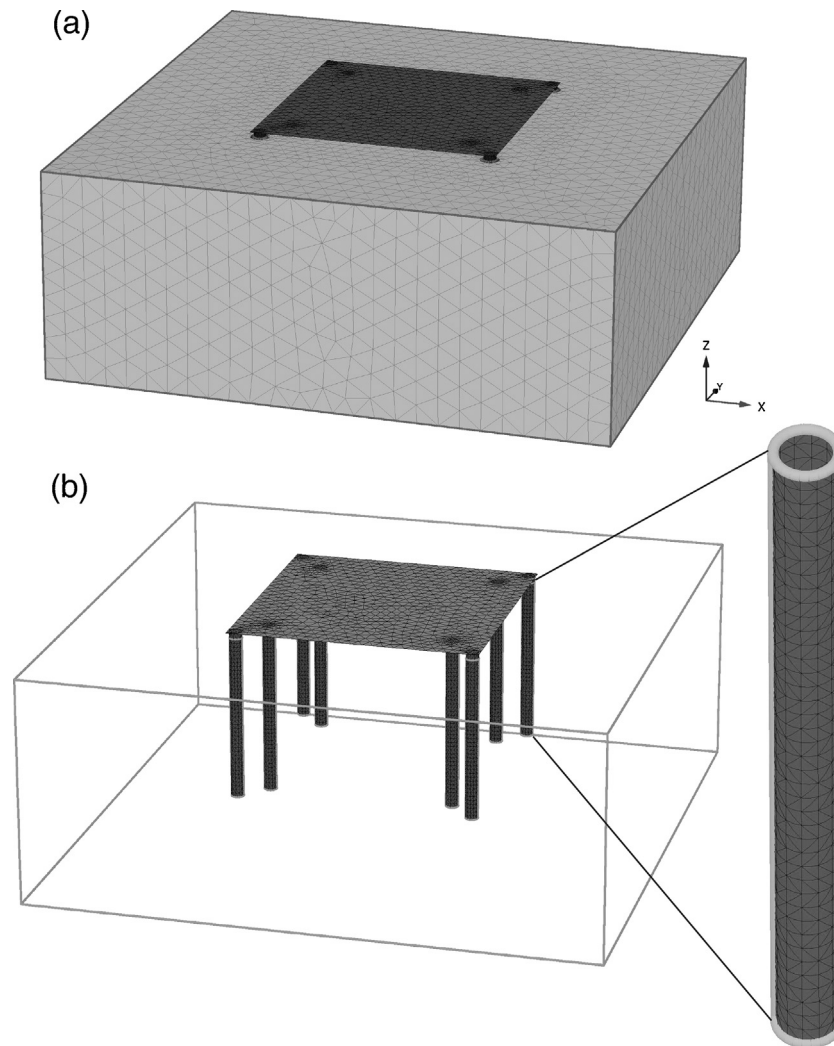


**Fig. 2.** Example of a finite element model used in the simulations:  $L = 12.5D$ ;  $S = 3D$  (a) Foundation system with soil; (b) typical mesh of closely spaced piles with upper plate and meshing detail of pile.

modeling the pile supporting system were placed in the model in the construction step. Interaction between the pile surfaces and the soil were activated with the predefined interface elements in this step. The interface shear strength was set to two-thirds of the soil's shear strength. In the third step, combined loading ( $V, H, M$ ) was applied.

### 3. Validation of the numerical model

In principle, the validity of the numerical model should be verified with experimental results prior to the parametric study. It was chosen to use large-scale field tests in order to validate the model instead of small-scale laboratory tests. The field test at Mustang Island [25] was used to validate the numerical model of a single pile. The reports based on large-scale fixed-head pile group tests are scarce in the literature. A closely spaced fixed-head two-pile field test carried out at Hollingside lane was used for the validation of the model developed for closely spaced double piles [26].

A back-calculation of pile test under static loading at Mustang Island near Corpus Christi, Texas, was carried out to validate the single pile numerical model [25]. The details of the test were reported in the studies of Reese et al. [25] and Reese and Van Impe [27]. The soil consisted of very dense sand with an averaged relative density  $I_D = 0.90$ , a friction angle  $\varphi' = 39^\circ$ , and a buoyant weight

$\gamma' = 10.37 \text{ kN/m}^3$ . The overall soil parameters considered for the back-calculation of the test are presented in Table 1. A driven open-ended steel pile with a diameter  $D_{ptest} = 0.61 \text{ m}$ , an embedded length  $L_{ptest} = 21 \text{ m}$  and a thickness  $t_{ptest} = 9.505 \times 10^{-3} \text{ m}$  was tested. The load was executed at  $0.305 \text{ m}$  above the mudline. An almost rigid plate was modeled at the pile head, and a horizontal load was applied to the center of the top plate to distribute the load uniformly onto the pile head. The load-pile head displacement relation of the field test results was compared with the results of numerical analysis, as presented in Fig. 4. The load-pile head displacement curve obtained by means of 3D finite element analyses of the field test was found to be in good agreement with the experimental curve.

Arta [26] investigated the response of laterally loaded single-pile and two-pile groups by performing a series of large-scale field tests at the Hollingside lane site. The group pile tests were implemented at various pile spacings and cap overhangs. Within the purpose of this study, a laterally loaded closely spaced double pile test with a three-pile width ( $S=3D$ ) spacing at  $h = 0.15 \text{ m}$  cap overhang was modeled for validation. The tests were performed in a sand trench. The trench was excavated with  $6 \text{ m} \times 1.2 \text{ m}$  plan dimensions and a depth of  $2.1 \text{ m}$ . Then, it was backfilled with compacted "yellow Permian sand". The compacted sand layer was underlain by "yellow firm clay". It was recorded that the water level was  $0.48 \text{ m}$ .

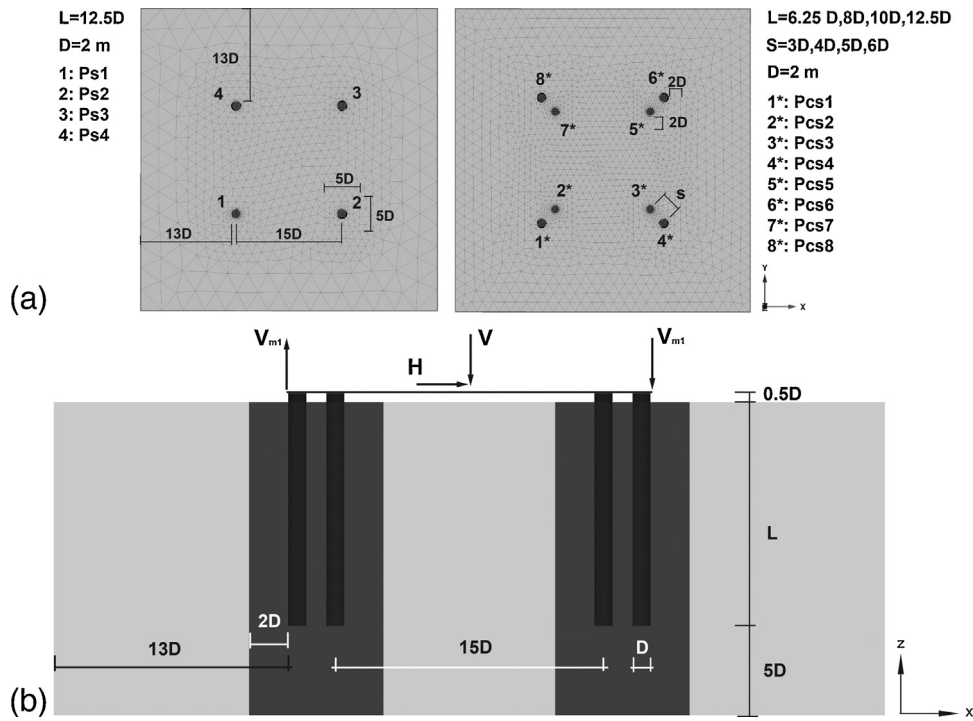


Fig. 3. Finite element model plan view, geometrical properties, and loading of foundation system: (a) Plan views of single-pile and closely spaced double-pile configurations; (b) Cross-section of closely spaced double-pile configurations.

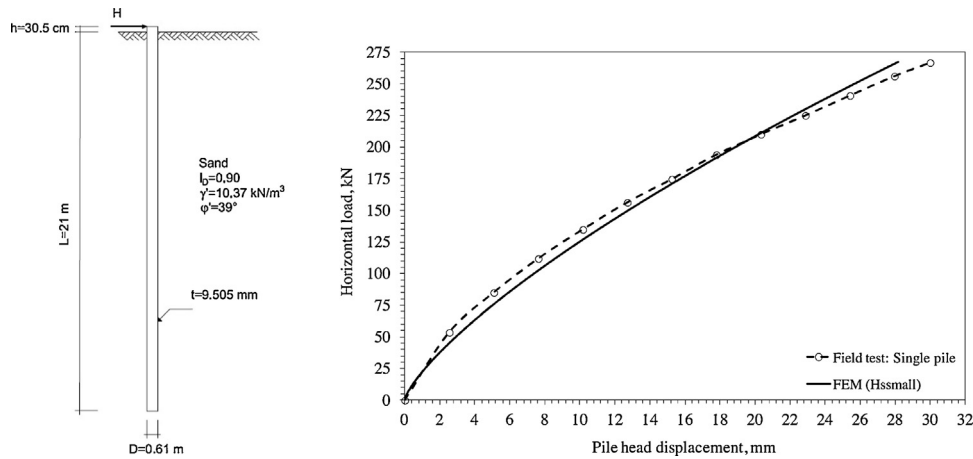


Fig. 4. Comparison of FEM and field test result for a single pile at 'Mustang Island'.

Table 2

Dense sand and firm clay parameters considered for the back-calculation of a fixed-head closely spaced double-pile field test at the "Hollingside lane site".

Parameter	Sand	Clay
Average unit weight, $\gamma$	18.70 kN/m <sup>3</sup>	20.00 kN/m <sup>3</sup>
Poisson's ratio, $\nu$	0.30 [-]	0.20 [-]
Power for stress level dependency of stiffness, m	0.65	0.50
Internal friction angle, $j'$	36.50°	18.0°
Dilation angle, $y$	6.50°	0°
Cohesion, $c'$	0.1 kN/m <sup>2</sup>	10 kN/m <sup>2</sup>
Initial void ratio, $e_{init}$	0.5 [-]	0.4 [-]
Secant stiffness in the standard drained triaxial test, $E_{50}^{ref}$	$6.0 \times 10^4$ kN/m <sup>2</sup>	$3.0 \times 10^4$ kN/m <sup>2</sup>
Tangent stiffness for primary oedometer loading, $E_{oed}^{ref}$	$3.97 \times 10^4$ kN/m <sup>2</sup>	$2.0 \times 10^4$ kN/m <sup>2</sup>
Unloading/reloading stiffness at engineering strains, $E_{ur}^{ref}$	$2.1 \times 10^5$ kN/m <sup>2</sup>	$0.9 \times 10^5$ kN/m <sup>2</sup>
Reference shear modulus at very small strains, $G_o^{ref}$	$1.35 \times 10^5$ kN/m <sup>2</sup>	$2.70 \times 10^5$ kN/m <sup>2</sup>
Shear strain at which, $G_s = 0.722G_o \cdot \gamma_{0.7}$	$0.1 \times 10^{-3}$ [-]	$0.12 \times 10^{-3}$ [-]
Failure ratio, $R_f$	0.90 [-]	0.90 [-]
Interface, $R_{inter}$	0.67 [-]	0.67 [-]

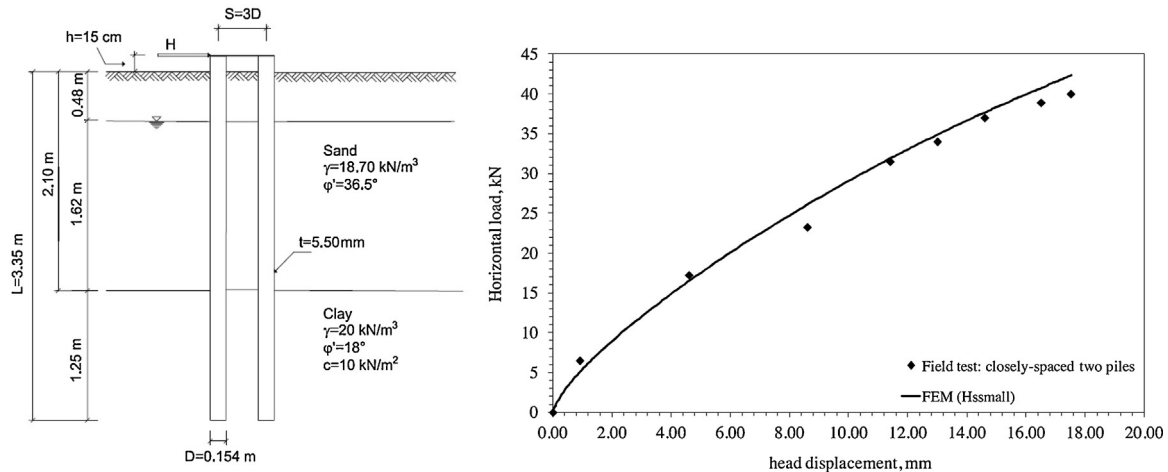


Fig. 5. Comparison of FEM and field test result for fixed-head closely spaced double-pile configuration at the “Hollingside lane site”.

The friction angle and average unit weight of the compacted sand were reported to be  $\phi' = 36.5^\circ$ ,  $\gamma = 18.70 \text{ kN/m}^3$ , respectively. Soil parameters of sand and clay considered for the back-calculation of field test is presented in Table 2. A hollow square pile with dimensions of  $0.154 \text{ m} \times 0.154 \text{ m}$ , thickness of  $t_{\text{ptest}} = 5.5 \times 10^{-3} \text{ m}$ , and an embedded length of  $3.35 \text{ m}$  was driven into the soil. The unit weight  $\gamma = 78 \text{ kN/m}^3$  was set for the pile portion above the water level. The pile heads were connected using a steel cap. An almost rigid plate was modeled for the cap. The determined numerical analysis-based load-head displacement relation was compared with the experimentally based result, as shown in Fig. 5. This comparison shows a good agreement of the numerical results with the field test results.

#### 4. Simulation results for reference systems

Detailed simulation results for the two reference systems are presented and discussed in this section. The reference systems consist of jackets supported by single piles with an embedded length of  $L = 25 \text{ m}$  ( $12.5D$ ) and jackets with closely spaced double piles with an embedded length of  $L/2 = 12.5 \text{ m}$  ( $6.25D$ ) in the case of a pile spacing of  $S = 5D$ , where the total length of all piles is same. The pile diameter  $D = 2 \text{ m}$  was set in the simulations, as mentioned in Section 2.

First, the results of the simulations of reference systems are presented in terms of the load-head displacement relation and the moment-head rotation relation (Fig. 6). The head displacement and rotation of the foundation system during the analyses were obtained by recording the horizontal displacement at the center of the upper plate and the vertical displacements of the upper plate edges, respectively. It can be seen from Fig. 6a that the lateral stiffness of the foundation with closely spaced double piles is considerably higher than that of the reference foundation with single piles. Utilizing a closely spaced double pile significantly reduced the head displacement, where the displacement reduction rate varies in a bandwidth of 33–52%. The moment-head rotation relation shows that the rotational stiffness of the jacket with closely spaced double piles was larger than that of the reference foundation with single piles, except the moment values  $M = 125 - 240 \text{ MNm}$  (Fig. 6c). The rotation reduction is noticeable, especially for further moment loads above  $M = 240 \text{ MNm}$ , which means that the reduction rate started to increase and reached a satisfactory level of 55%. The results show that the response of the jacket supported by closely spaced double piles with a pile spacing of  $S = 5D$  is superior to that of the jacket supported by a single pile, although the total length of the piles is same.

The simulations for the reference systems were conducted under  $H = 11 \text{ MN}$  horizontal loading in order to reach large head displacements and capture the response towards the ultimate load capacity  $H_u$ . The hyperbolic method suggested by Manoliu et al. [28] was used for this purpose. The ultimate load capacity is defined as the inverse slope of the linear part of the  $y/H$  to  $y$  relationship in this method as shown in Fig. 6b. Consequently, it was obtained that the ultimate horizontal load capacity of the reference jacket with closely spaced double piles ( $H_u = 17.09 \text{ MN}$ ) was approximately 15% larger than that of the reference foundation with single piles ( $H_u = 14.90 \text{ MN}$ ).

The efficiency of individual piles is affected by pile spacing due to overlapping of the resisting zones. Because closely spaced piles are displaced, the resistance zones for the individual piles overlap. Although the displacement of the piles in group is the same due to the fixed head condition, there is a tendency for the trailing pile (back) to display less resistance than the leading pile (front) as a result of “shadowing” and pile-soil-pile interaction, as illustrated in Fig. 7. The effective stress ( $\sigma'_{xx}$ ) derived from at the load stage  $H = 8 \text{ MN}$  is applied in the parametric study at a depth of  $z = 5 \text{ m}$  for the reference systems is presented in Fig. 8. It can be seen from Fig. 8a that the stress overlapping did not take place in the active zone of loaded jacket with single piles due to enough large pile-spacing ( $S = 15D$ ). Conversely, Fig. 8b reveals that the overlapping of stress zones occurred between each leg of the double piles ( $S = 5D$ ).

The results presented in Fig. 8 indicate that the soil reaction is related to pile spacing because of a “shadow-effect”. Hence, the “shadow-effect” varies the distribution of the total load to each pile when the piles are installed close to each other. In addition, the distribution of the total load to each pile depends on the position of the pile in the closely spaced pile configuration. In this study, the closely spaced double piles were arranged diagonally for each leg of the jacket foundation. In this diagonal design, it is expected that the leading (front) and trailing (back) piles, according to the loading direction, carry different loads due to overlapping stress zone phenomena. To determine the load distribution to each pile, the soil reaction along the pile length was evaluated at the load stage  $H = 8 \text{ MN}$ . The soil reaction was determined using the method of extracting stress data from the interface elements, which is well documented in the study of Ibsen et al. [29]. Stress extraction from the nearby soil elements and interface element methods were compared, and consequently, it is stated that the best response is acquired by extracting the data from the interface [29].

The stresses were extracted at  $0.5 \text{ m}$  intervals along the pile, and only the lateral resistance of the soil was considered. For this purpose, the effective normal stress ( $\sigma'_N$ ) acting normal to the

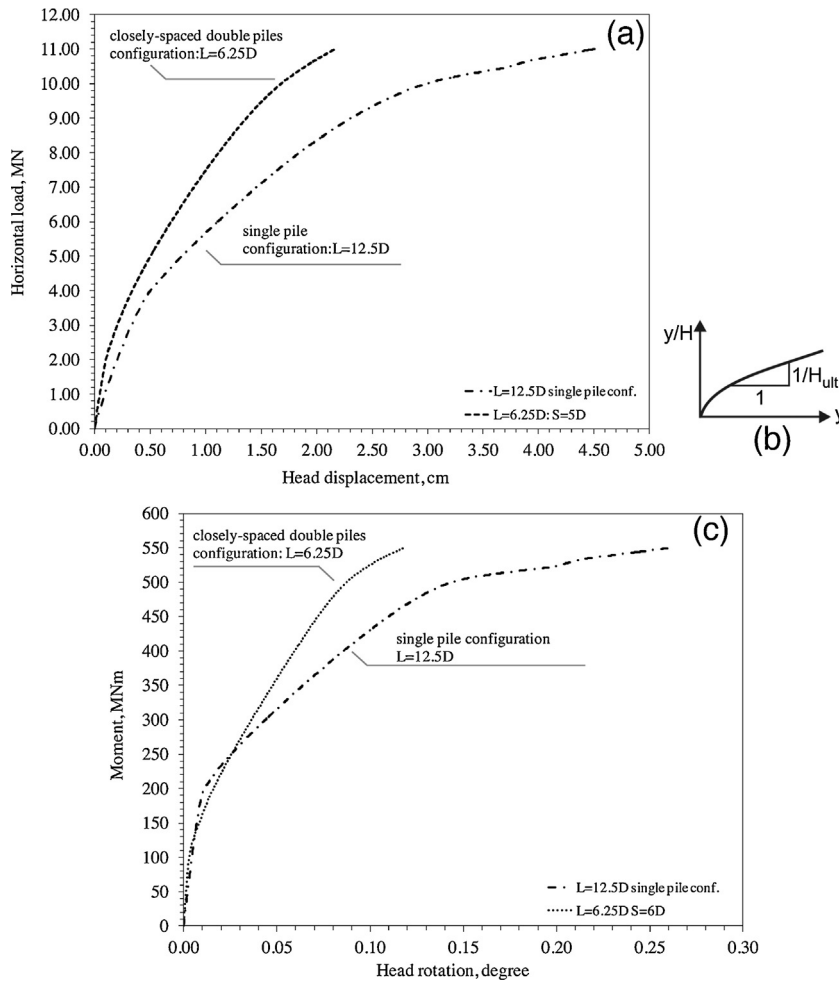


Fig. 6. Horizontal load-head displacement and moment-head rotation relations for the reference systems.

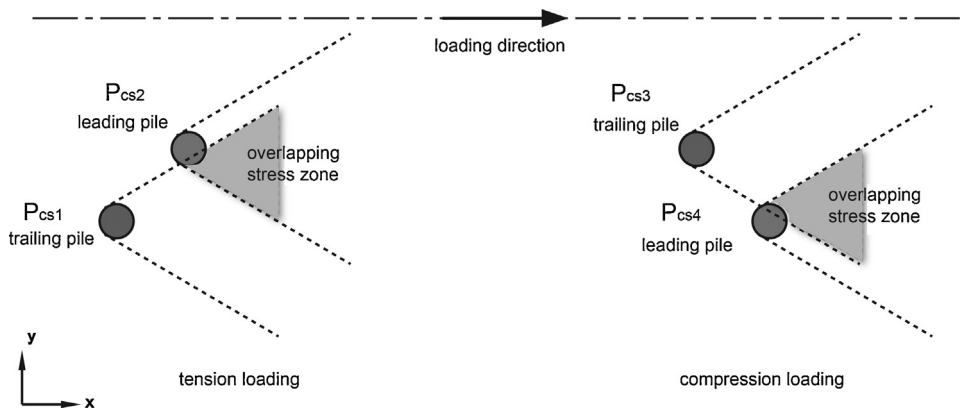


Fig. 7. Illustration of overlapping stress zones for closely spaced double-pile configuration.

interface surface and the shear stress ( $\tau_1$ ) acting along the circumference of the pile data was extracted from the FE model. Then, considering the horizontal loading direction, the soil reaction was obtained with the sum of the computed x-component of the stresses ( $\sigma'_N, \tau_1$ ). The shear stress acting vertically along the pile length ( $\tau_2$ ) was not taken into consideration in this study. To validate the method, the stress extraction process was applied to the reference single pile configuration model. It can be seen from Fig. 9 that the soil reaction along the pile depth was quite similar for each pile, where the spacings of the piles (15D) are large enough. The sum

of the lateral soil reactions along the pile, which means the load carried by each pile, was found to be  $P_{s1} = 1.95MN$ ;  $P_{s2} = 2.00MN$ ;  $P_{s3} = 2.01MN$ ;  $P_{s4} = 1.94MN$ , which implies that the distribution of the total lateral load to each pile is quite equal. Moreover, the total lateral soil reaction (carried load) obtained from the FE analysis within the extraction data method  $\sum H = 7.9MN$  was sufficiently approximated (99%) to the applied horizontal loading ( $H = 8MN$ ).

For jacket foundations, the moment loading arising from horizontal load eccentricity is transferred to vertical loads consisting of tension and compression on the individual piles depending on



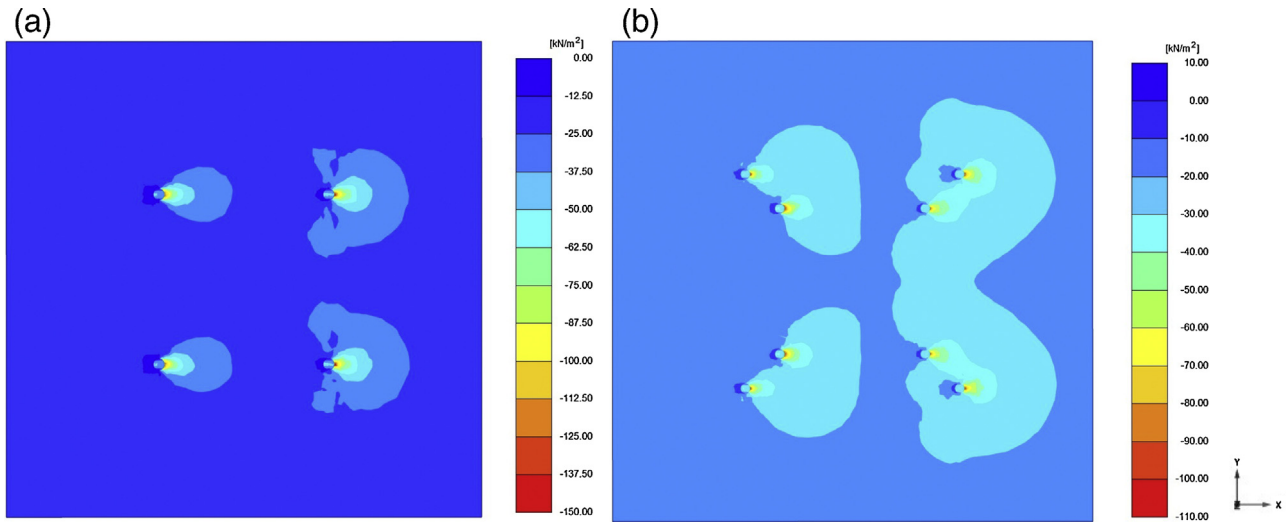


Fig. 8. Effective stress ( $\sigma'_{xx}$ ) derived from at the final load stage at a depth of  $z = 5$  m for the reference systems.

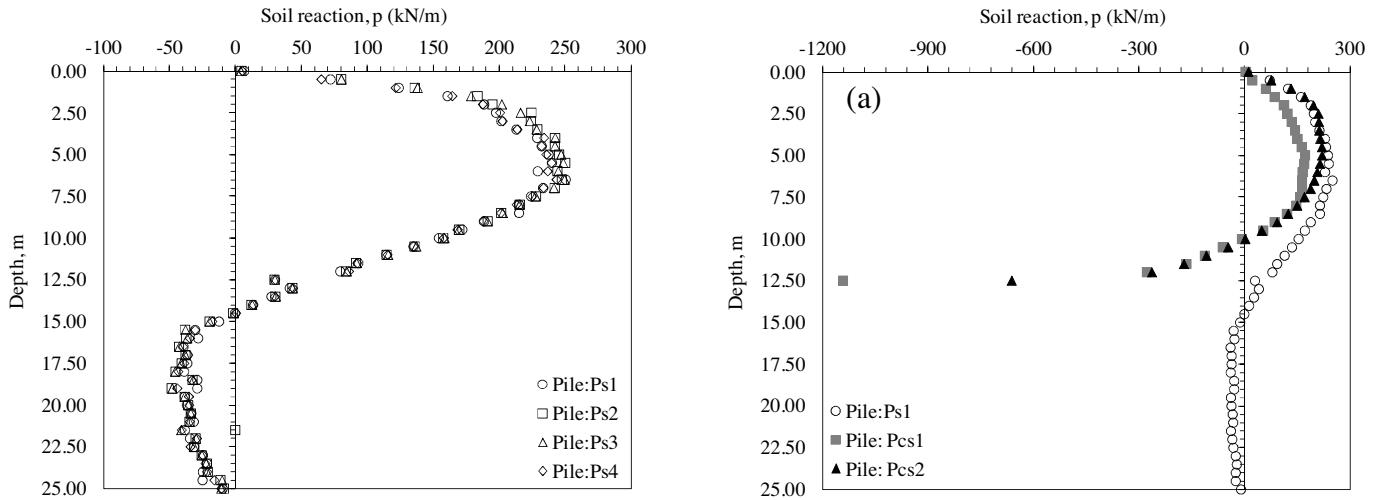


Fig. 9. Soil reaction along the piles for reference single pile configuration ( $L = 12.5D$ ,  $D = 2$  m).

the direction of the load. According to the load distribution results, the piles on the tension loading side, Ps1 and Ps4, carried 49% and the piles on the compression loading side, Ps2 and Ps3, carried 51% of the total applied load, which shows that the effect of the load distribution among the piles on the compression and tension sides is insignificant in the single-pile configuration.

Soil reactions along the pile depth of the reference systems are compared and presented in Fig. 10. The figure indicates that the soil reaction along the pile strongly depends on the pile length (Fig. 10). The response of the soil reaction achieved in the reference jacket with closely spaced double pile configuration designed with length  $L/2$  for each pile is considerably different from the soil reaction-depth relation of the single pile designed with pile length  $L$ . It should be noted that the reactions in the tension piles were obtained noticeably different from those of the compression piles (Fig. 10). The results show that overlapping of soil resistance significantly affected the soil reaction of tension piles (Pcs1; Pcs2) and slightly affected the soil reaction of compression piles (Pcs3; Pcs4). In the tension piles, the soil reaction along the depth of the trailing pile is apparently less than that of the leading pile (Fig. 10a).

According to load distribution results, the tension piles Pcs1 and Pcs2 carried 40% and compression piles Pcs3 and Pcs4 carried 60%

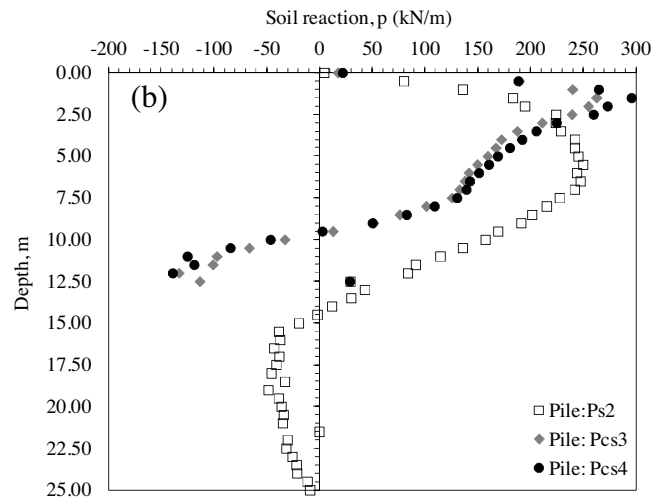


Fig. 10. Comparison of soil reactions along the pile depths of reference systems at the end of the last loading step.

of the total applied lateral load, which shows that the effect of load distribution among the piles on the compression and tension sides is significant in the closely spaced double-pile configuration. The result indicates that the horizontal stiffness of the tension piles is smaller than that of the compression piles in the closely spaced double-pile configuration.

5. Parametric study

The contribution of utilizing closely spaced double piles on the response of the jacket foundation was investigated in this study. The second essential goal of the research is to investigate the distribution of the total load to each pile in the closely spaced double pile configuration. Therefore, a parametric study was executed for the conventional pile-supported jacket and closely spaced double-pile-supported foundation systems. Various pile spacings ( $S : 3D, 4D, 5D, 6D$ ) and embedded pile lengths ( $L : 6.25D, 8D, 10D, 12.5D$ ) were modeled in the closely spaced piled configuration, and its response was compared with that of the reference jacket supported with single piles ( $L = 12.5D$ ), where  $D=2\text{ m}$  is the diameter of the pile.

5.1. Effect of pile spacing and pile length on the behavior of the foundation system

The effect of the pile length and pile spacing on the load-head displacement relation, the moment-head rotation relation, and initial stiffness of the foundation system are presented in the following paragraphs.

The load-head displacement and the moment-head rotation relations were obtained from the parametric study, as shown in Fig. 11. According to Fig. 11a, the displacements significantly decreased in the configuration of closely spaced double piles, which implies a stiffer behavior in comparison with the single-pile configuration. The same manner was observed in the comparison of the moment-head rotation relations in general (Fig. 11b). Rotations of the closely spaced double-pile jacket were apparently less than those of the single-pile-supported jacket with the increase of the moment, especially for foundations with pile lengths  $L = 8D, 10D, 12.5D$ . An exception was found for the rotations of closely spaced double pile configuration with an embedded length  $L/2 = 12.5\text{m} (6.25D)$ . In a particular range of moments depending on the pile spacing, rotations were obtained that were larger than those of the single-pile configuration, i.e., between the moments  $M = 100 - 270\text{MNm}$  for pile-spacing  $S : 3D$ . The above-mentioned moment range and the increase in the rotation decreased with the increase in the pile spacing. For instance, the rotations slightly increased between the moments  $M = 125 - 215\text{tm}$  for the pile spacing  $S = 6D$ .

It should be noted that the displacements and rotations significantly decrease with increases in the pile length in the closely spaced pile configuration. This implies that the load-head displacement and the moment-head rotation are strongly dependent on the pile length. The effect of the pile spacing on the load-head displacement and the moment-head rotation were secondary but still notable, especially for the pile lengths  $L = 10D, L = 8D$ , and  $L = 6.25D$ . The behavior of the double-pile configuration with pile length  $L = 12.5D$  shows a very rigid behavior and was slightly affected by the pile spacing.

The displacement reduction ( $R_y$ ) and rotation reduction ( $R_\theta$ ) factors were obtained according to the load-head displacement and moment-head rotation relations. The factors determination method is shown in Fig. 12. The  $R_y$  and  $R_\theta$  factors can be defined as the ratios of the displacement  $y_{cs}$  and rotation  $\theta_{cs}$  of the closely

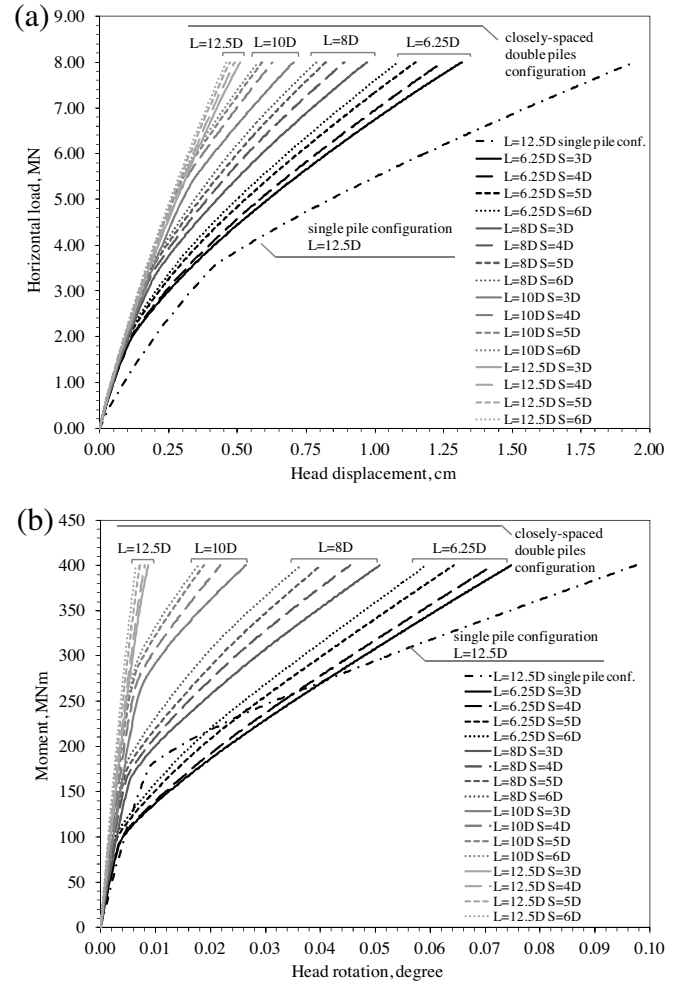


Fig. 11. Horizontal load-head displacement and moment-head rotation relations.

spaced double-pile configuration to the displacement  $y_s$  and rotation  $\theta_s$  of the single-pile configuration, respectively:

$$R_y = \frac{y_{cs}}{y_s} \tag{1}$$

$$R_\theta = \frac{\theta_{cs}}{\theta_s} \tag{2}$$

The relations of the displacement reduction factor to the horizontal load ( $R_y - H$ ) and the rotation reduction factor to the moment ( $R_\theta - M$ ) are presented in Fig. 13. The initial stiffness which is considered approximately linear and the transition to nonlinear soil response are indicated in Fig. 12. It should be noted that the transition to nonlinear soil response have a large influence on the characteristics of the  $R_y - H$  and  $R_\theta - M$  curves. In other words, the characteristics of the curves vary with an increase in the horizontal load. The curves in all cases change abruptly at the particular horizontal load level  $H \cong 3.60\text{MN}$  (Fig. 12), which corresponds to the transition to nonlinear soil response of the reference single-pile configuration, which is shown by a vertical dashed line in the figure. The  $R_y$  and  $R_\theta$  factors decrease in general with increases in the horizontal load in the cases  $L = 12.5D, L = 10D$ , and  $L = 8D$ . In other words, the reduction rates for the displacements and rotations increase. The characteristics of the  $R_y - H$  and  $R_\theta - M$  curves are quite different from the other curves in the case  $L = 6.25D$ . In the case  $L = 6.25D$ , the  $R_y$  and  $R_\theta$  factors changed slightly up to the transition to nonlinear soil response  $H \cong 1.80\text{MN} - 1.95\text{MN}$ . Afterwards, the factors almost linearly increase up to a horizontal load

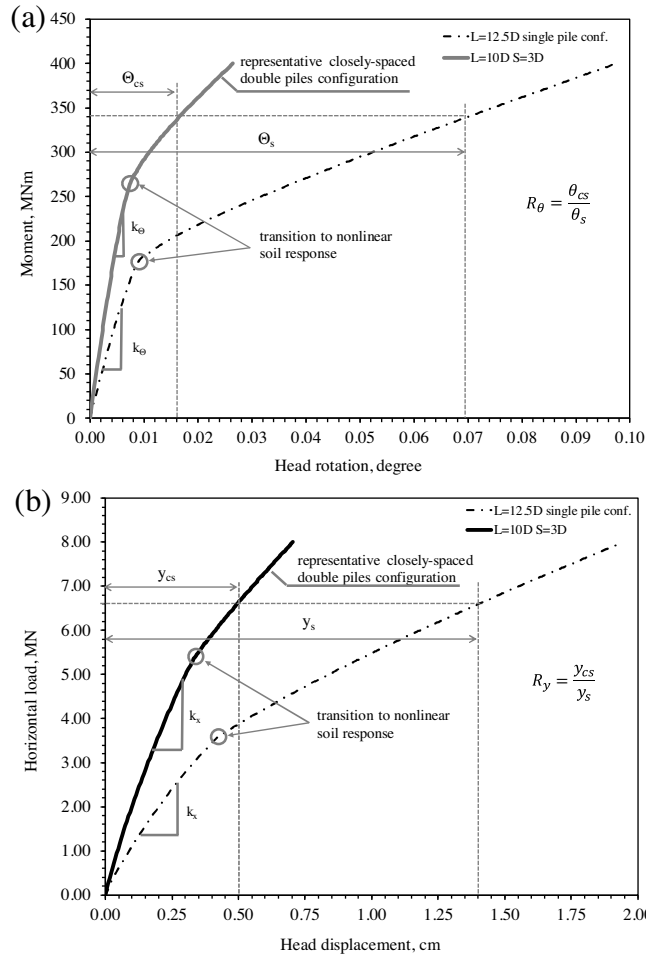


Fig. 12. Displacement and rotation reduction factors determination method.

$H \cong 3.60MN$  and then decrease parabolically in further loadings (Fig. 13).

When focusing on the double-pile configuration with  $L = 8D$ , it can be seen that the displacement reduction factor varies with a bandwidth of  $R_y = 0.57 - 0.40$  or a reduction rate of 43 – 60% for various horizontal loads and pile spacings, which is significantly high. The factor  $R_y$  varies from 0.81 to 0.50 with a reduction rate of 19 – 50% for the shortest pile configuration  $L = 6.25D$ . The  $R_\theta$  factors in the configuration with pile length  $L = 8D$  are considerably less than those in the configurations with pile lengths of  $L = 12.5D$  and  $L = 10D$ . Moreover, for the  $L = 8D$  configuration, the rotation reduction factor varies in a bandwidth  $R_\theta = 0.98 - 0.55$ . In other words, the rotation reduction rate varies between 2 and 45% for various moments and pile spacings, which is also remarkable. For the shortest pile configuration,  $L = 6.25D$ , the rotation reduction factor obtained was more than  $R_\theta > 1.00$  between the particular moment ranges (i.e.,  $M = 100 - 270MNm$  in the case  $S = 3D$  and  $M = 125 - 215MNm$  in the case  $S = 6D$ ), which indicates an increase of rotation. It can be seen that the moment range where an increase in the rotation occurs is reduced with an increase in the pile spacing. Apart from the moment range  $M = 125 - 215MNm$ , the obtained rotation reduction factors reach  $R_\theta = 0.51$ , which corresponds to a rotation reduction rate of 49% in the case with  $L = 6.25D$  and  $S = 6D$ .

The results show that  $R_y - H$  and  $R_\theta - M$  relations are strongly dependent on the pile length. The  $R_y$  and  $R_\theta$  factors considerably decrease with an increase in the pile length with identical pile spacings. Moreover, the  $R_y$  and  $R_\theta$  factors decreases with an increase

in the pile spacing. It was observed that the influences of pile spacing on the reduction factors are more effective in the shortest pile configuration than the others.

The stiffness under small (operational) loads is an essential aspect in the design of offshore wind energy foundations because initial stiffness affects the natural frequency of the wind energy tower. Therefore, the effect of the pile spacing and the pile length on the initial stiffness of the single-pile and closely spaced double-pile configurations for the foundation were also focused on in the executed parametric study. For this purpose, in addition to the reference system, the initial stiffness of single pile configuration with pile length  $sL = 8D$ ,  $L = 10D$ , and  $L = 6.25D$  were also determined.

The initial lateral stiffness ( $k_x$ ) and rotational stiffness ( $k_\theta$ ) were obtained according to the normalized pile spacing, as shown in Fig. 14, where  $k_x$  and ( $k_\theta$ ) can be defined as follows:

$$k_x = \frac{\Delta H}{\Delta y} \tag{3}$$

$$k_\theta = \frac{\Delta M}{\Delta \Theta} \tag{4}$$

It can be seen from Fig. 14 that the initial lateral stiffness is slightly dependent on the pile length but significantly dependent on the pile spacing. The initial rotational stiffness  $k_\theta$  is significantly dependent on both the pile length and the pile spacing. A visible increase in  $k_\theta$  was obtained with an increase in the pile length and pile spacing in general (Fig. 14).

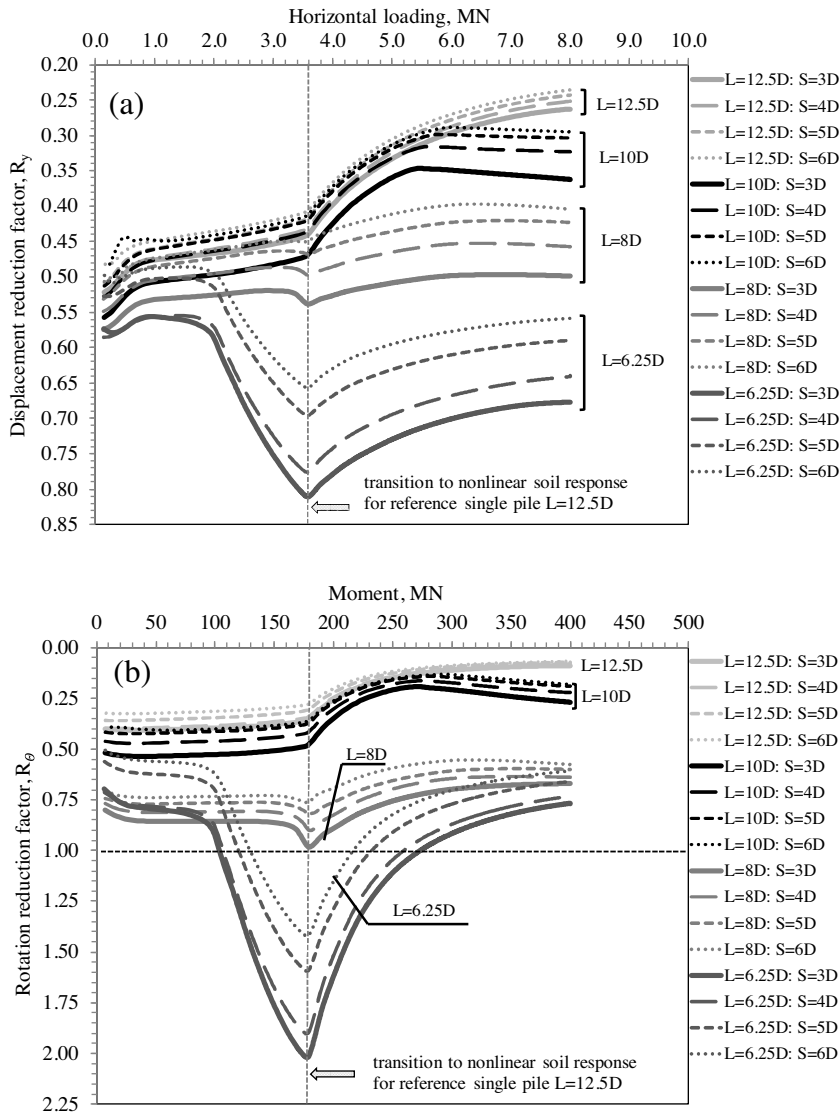


Fig. 13. Displacement reduction factor–horizontal loading and rotation reduction factor–moment relations.

5.2. Effect of pile spacing and pile length on the load distribution

After the validation of the stress extraction method expressed in Section 4, the total load distribution to the each pile was obtained for closely spaced double piles configuration according to the parametric study. The load distribution factor  $f_{Ld}$  was determined from the ratio of the soil reaction to the applied lateral load at the final load stage divided by the number of piles. The factor  $f_{Ld}$  was obtained to compare the load carried by each pile and evaluate the effect of pile-spacing and pile length on the load distribution (Eq. (6)):

$$L_p = f_{Ld} \times \frac{1}{n} \times p_t \tag{6}$$

Here,  $L_p$  indicates the load carried by each pile;  $f_{Ld}$  is the load distribution factor;  $p_t$  is the total soil reaction or total load and  $n$  describes the number of piles ( $n = 8$ ;  $\frac{1}{n} = 0.125$ ) in the configuration.

The load distribution factor  $f_{Ld}$  versus normalized pile spacing ( $S/D$ ) is presented for each pile in Fig. 15. The  $f_{Ld} - (S/D)$  relations of the piles on the compression and tension loading sides are presented in detail in Fig. 15c and Fig. 15d, as the tension and compression loadings arising from the moment differently affect the

relation. The piles in compression loading side and tension loading side are defined as compression piles and tension piles in this study (Fig. 15b). Considering the symmetry of the x-axis, the pile pairs Pcs1 and Pcs8, Pcs2 and Pcs7, Pcs3 and Pcs5, and Pcs4 and Pcs6 have identical value load distribution factors (Fig. 3). Therefore, the subsequent evaluations are made for the piles Pcs1, Pcs2, Pcs3, and Pcs4, which are also valid for the corresponding piles in symmetry.

First, the load distribution factor  $f_{Ld}$  is strongly dependent on the pile length according to the results. Second, tension loading and compression loading have a significant influence on the  $f_{Ld}$ . Third, the position of the pile, leading pile and trailing pile for both the tension piles and compression piles considerably changed the load distribution factor  $f_{Ld}$ . While the pile-spacing has almost no influence on the load distribution factor of the tension piles (Fig. 15c), the factors of compression piles are noticeably affected by the pile spacing (Fig. 15d).

The results show that the factors  $f_{Ld}$  of the leading piles are evidently higher than the factors of trailing piles in all cases in tension piles (Fig. 15c). The factors of the leading piles are found to be 2.2–6.9%, 15–18%, 42–47%, and 83–95% higher than those of the trailing piles on the tension loading side for the cases with  $L = 12.5D$ ,  $L = 10D$ ,  $L = 8D$ , and  $L = 6.25D$ , respectively. It is

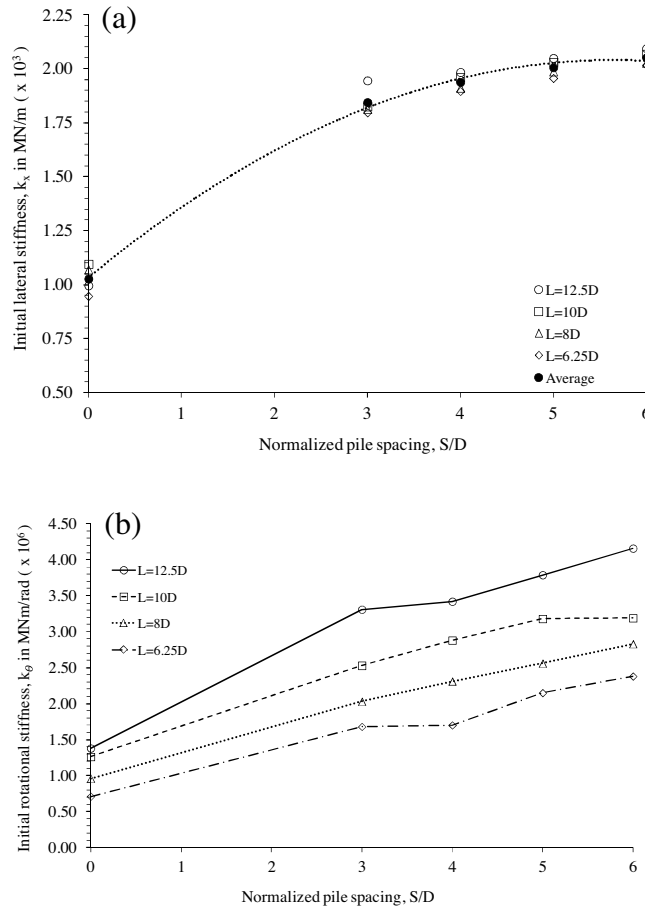


Fig. 14. Initial lateral stiffness-normalized pile spacing and initial rotational stiffness-normalized pile spacing relations.

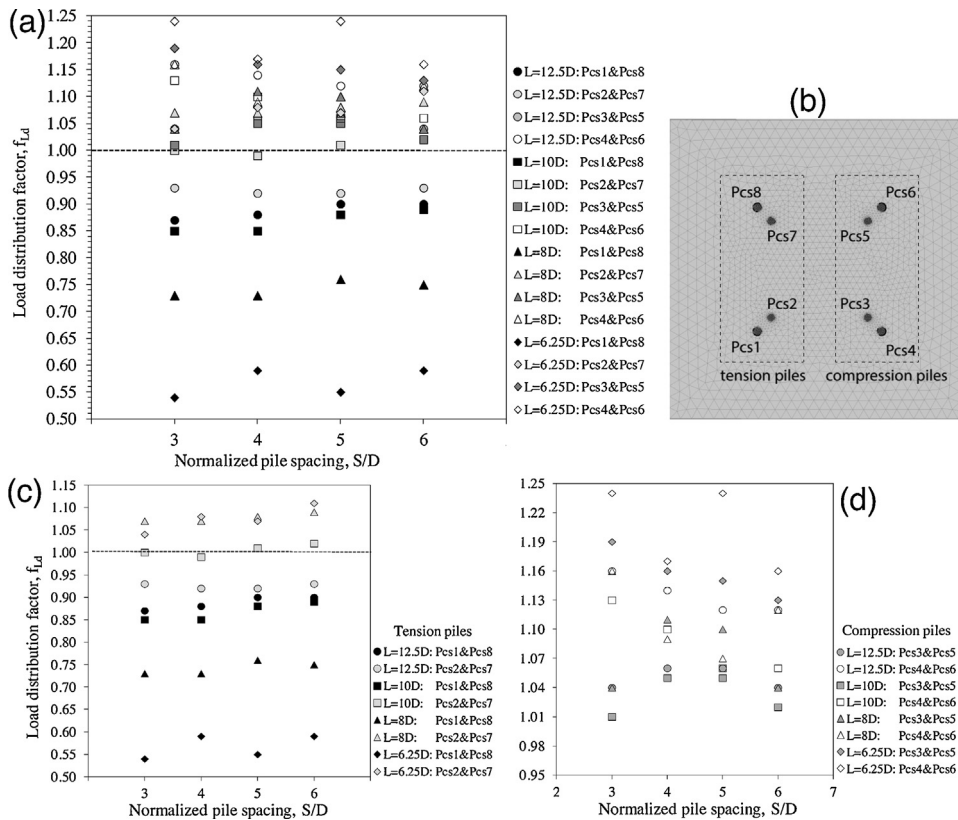


Fig. 15. Load distribution factor- normalized pile spacing relations.

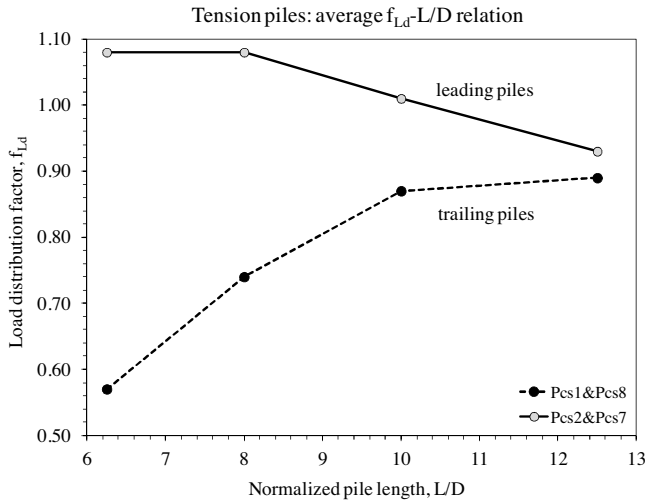


Fig. 16. Average load distribution factor-normalized pile length relations in tension piles.

possible to present the relation of the average load distribution factor to the normalized pile length  $f_{Ld} - (L/D)$  for tension piles with various lengths (Fig. 16), as the factors are nearly independent of the pile-spacing, as can be seen in Fig. 15c. The results indicate that the shorter the pile is, the greater is the difference between the factors for the tension piles.

In the compression loading side, the load distribution factors of the leading piles were slightly higher than the factors in the trailing piles: 1–12% except in the case  $L = 8D$ ;  $S = 4D$ ,  $S = 5D$ , where the factors of the leading piles were found to be slightly smaller than those of the trailing piles (Fig. 15d).

The load distribution factors of the trailing piles on the compression loading side are considerably higher than those on the tension loading side, i.e., between 92 and 120% in the case  $L = 6.25D$ . Conversely, the load distribution factors of the leading piles on the compression loading side are moderately higher than those on the tension loading side, i.e., between 4.5 and 19% in the case  $L = 6.25D$ .

It should be noted that the load distribution factors were larger than one, that is,  $f_{Ld} > 1.00$ , for the piles (Pcs3 and Pcs4) on the compression loading side (Fig. 15d), which implies that the piles carried more load than the tension piles; this is in line with the findings of Achmus and Thieken [10]. The average load carrying distribution according to the normalized pile length ( $L/D$ ) relation is shown in Fig. 17. The results show that the compression piles Pcs3 and Pcs4 together carried more load (59% for shortest pile – 53%) than the sum of the load carried by tension piles Pcs1 and Pcs2 (41% for shortest pile – 47%). According to the average load distribution results, the leading piles, Pcs4 and Pcs6, carried an average of 51% and the trailing piles, Pcs3 and Pcs5, carried an average of 49% of total load on the compression side. The results indicate that the load carrying distribution of the compression piles on average is slightly dependent on the pile length (Fig. 17). Conversely, the average load-carrying distribution between the leading and trailing piles on the tension loading side is strongly dependent on the pile length, and with an increase in the pile length, the difference decreases. While the leading pile carried 65% and the trailing pile carried 35% of total load on the tension side in shortest pile case, with  $L = 6.25D$ , the carrying load distribution was found to be 51% and 49% for longest pile case, with  $L = 12.5D$  (Fig. 17). Consequently, the leading piles, Pcs2 and Pcs4, carry more load than the trailing piles, Pcs1 and Pcs3, on both the compression and tension sides in almost all simulations due to overlapping of the resisting zones.

Finally, the results indicate that tension loading significantly affected the load distribution factor. The load distribution

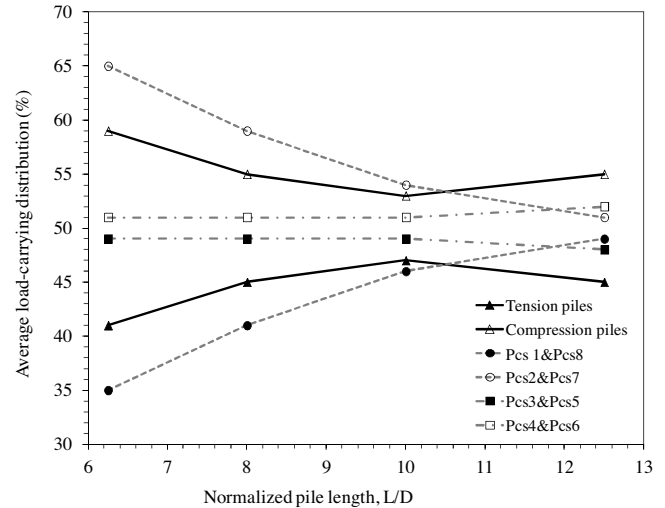


Fig. 17. Average load-carrying distribution-normalized pile length relations.

factors of the tension piles were determined to be less than those of the compression piles, which implies that the piles on the tension-loading side carried considerably less load than the piles on the compression side. Moreover, the position of the piles is more important on the tension side because the difference in the factors between trailing and leading piles on the tension side evidently contributed more than the compression piles. This shows that the “shadow effect” evidently occurs, especially for the piles on the tension loading side. It is revealed from all of these results that combined tensile loading caused a reduction in the horizontal soil-pile stiffness. During the uplift of the pile, due to the combined tension loading, the soil-pile stiffness is reduced. The shear stresses acting around the pile occurred in an upward direction because the tension loading reduced the mobilizable passive earth pressure. Similar findings were also reported in the study of Achmus and Thieken [10] related to the behavior of piles under combined tensile loading. These researchers stated that the reduction in the system stiffness is caused by the negative influence of skin friction stresses on the mobilizable passive earth pressure. This response is more visible in the analysis results of the shortest pile with  $L = 6.25D$ . The shorter the pile is, the greater the effect is on the load distribution factor between the leading and trailing piles on the tension loading side. The resistance to the tension load decreases, and the shortest pile is rotated and moves up more than the other piles. Moreover, the trailing piles subjected more tension load than the leading piles, which resulted in a great reduction in the system stiffness. Therefore, the load distribution factors of the trailing piles were determined to be less than those of the leading piles.

## 6. Conclusions

A numerical-based parametric study was carried out for a novel supporting system consisting of a jacket with closely spaced double piles for large offshore wind energy converters in deep waters. The effects of pile spacing and embedded pile length on the response of the foundation and load distribution among the piles were investigated. The response of the foundation was investigated in the context of load-head displacement and moment-head rotation relations, rotation and displacement reduction factors, and initial lateral and rotational stiffness. The ultimate horizontal load capacity was found for only the reference foundation systems. The influence of pile spacing and pile length on the ultimate

capacity will be evaluated in the further studies. The following main conclusions can be drawn from the results:

- The back-calculation of large-scale field tests consisting of single-pile and closely spaced fixed-head double-pile tests reported in the referenced literature indicated that the response of these foundation systems in sand under monotonic loading can be well simulated using the hardening soil model with a small strain stiffness (HSsmall).
- The results show that stress extraction from interface elements is an efficient method [29], as the total lateral soil reaction along the pile acquired from the FEM was sufficiently approximated to the applied head horizontal loading.
- It can be revealed from the results that the response of the foundation with closely spaced double piles is generally considerably stiffer than the reference foundation system with single piles with respect to the load-head displacement and the moment-head rotation results.
- It is remarkable that designing a jacket foundation with closely spaced piles with an embedded length of  $L/2$  and a pile spacing of  $S$  ( $S = 5D, 6D$ ;  $D$ : pile diameter) provides a significantly better response in the above-mentioned context than the response of a single-pile configuration with embedded length  $L$ , although the total length of the piles is same.
- It was obtained that the ultimate horizontal load capacity of the reference jacket with closely spaced double piles ( $L/2 = 12.5m(6.25D$  and  $S = 5D)$ ) was approximately 15% larger than that of the reference foundation with single piles ( $L = 25m(12.5D)$ ).
- The parametric study results show that the responses of the foundation and load distribution to each pile are strongly dependent on pile length and remarkably dependent on pile spacing. The shorter the pile is, the greater the effects of the pile length and pile spacing on the specified relations and factors are.
- In contrast, the initial lateral stiffness is nearly independent of the pile length.
- Pile spacing has almost no influence on the load distribution factor of tension piles.
- Tension loading considerably affected the load distribution factor. The piles on the tension loading side carried clearly less load than the piles on the compression side. It is revealed that combined tensile loading caused a reduction in horizontal soil-pile stiffness.
- The position of the piles becomes more important on the tension side, as the trailing piles carried considerably less load than the leading piles.
- The difference in the factors between trailing and leading piles on the compression piles is small. This shows that the “shadow effect” evidently occurs, especially for the piles on the tension loading side.

This parametric study enables us to understand the behavior of the recommended supporting system designed with closely spaced double piles and to estimate its load distribution among the piles. The results of the study were presented with various parameters or factors to estimate the design of a foundation for offshore structures with closely spaced double piles in very dense sand. It is concluded that the recommended configuration enables the reduction of each pile length and the considerable improvement of the load-bearing behavior of the system. It should be noted that further research is needed at various soil relative densities, horizontal load levels and experimental and numerical investigation under cyclic loadings.

### Acknowledgments

The author highly appreciates Dokuz Eylül University, Department of Civil Engineering, for providing finite element analysis software.

### References

- [1] E. Hau, *Wind Turbines: Fundamentals, Technologies, Application, Economics*, 3rd ed., Springer, Berlin, 2013.
- [2] The European Wind Energy Association (EWEA), *Deep Water: The Next Step for Offshore Wind Energy* Brussels, The European Wind Energy Association, 2013.
- [3] B.W. Byrne, G.T. Houlsby, Foundation for offshore wind turbines, *Philos. Trans. R. Soc. A* 361 (2003) 2909–2930.
- [4] M. Achmus, C.T. Akdag, K. Thieken, Load-bearing behavior of suction bucket foundations in sand, *Appl. Ocean Res.* 43 (2013) 157–165.
- [5] E. Tasan, S.A. Savidis, C.T. Akdag, Pore water pressure development around the monopile foundations of offshore wind energy converters (in Turkish with English Abstract), *J. Faculty Eng. Archit.* 29 (2014) 331–341.
- [6] S.-R. Kim, L.C. Hung, M. Oh, Group effect on bearing capacities of tripod bucket foundations in undrained clay, *Ocean Eng.* 79 (2014) 1–9.
- [7] C. Lupea, R. Thijssen, F. van Tol, Long term effects of cyclic loading on suction caisson foundations in sand, *Geotechniek* 1 (2014) 18–24.
- [8] W. Shi, H. Park, C. Chung, J. Baek, Y. Kim, C. Kim, Load analysis and comparison of different jacket foundations, *Renew. Energy* 54 (2013) 201–210.
- [9] M. Achmus, K. Abdel-Rahman, F. tom Wörden, Geotechnical design of piles supporting foundation structures for offshore wind energy converters, in: J.S. Chung, S.W. Hong, S. Nagata, A.J.N.A. Sarmento, W. Koterayama (Eds.), *Proceedings of the Sixteenth International Offshore and Polar Engineering Conference*, International Society of Offshore and Polar Engineers (ISOPE), Lisbon, 2007, pp. 322–327.
- [10] M. Achmus, K. Thieken, On the behavior of piles in non-cohesive soil under combined horizontal and vertical loading, *Acta Geotech.* 5 (2010) 199–210.
- [11] C.T. Akdag, G. Özden, Nonlinear behavior of reinforced concrete (RC) and steel fiber added RC (WS-SFRC) model piles in medium dense sand, *Constr. Build. Mater.* 48 (2013) 464–472.
- [12] K. Lensy, J. Wiermann, Design aspects of monopiles in German offshore wind farms, in: S. Gourvenec, M. Cassidy (Eds.), *Frontiers in Offshore Geotechnics*, Taylor & Francis Group, London, 2005, pp. 383–389.
- [13] A.H. Augustesen, C.T. Leth, M.U. Østergaard, M. Møller, J. Dührkop, P. Barbosa, Design methodology for cyclically and axially loaded piles in chalk for Wikingen OWF, in: V. Meyer (Ed.), *Frontiers in Offshore Geotechnics*, Taylor & Francis Group, London, 2015, pp. 509–514.
- [14] M. McVay, R. Casper, T. Shang, Lateral response of three-row groups in loose to dense sands at 3D and 5D pile spacing, *J. Geotech. Eng.-ASCE* 121 (1995) 436–441.
- [15] M.C. Papadopoulou, E.M. Comodromos, On the response prediction of horizontally loaded fixed-head pile groups in sands, *Comput. Geotech.* 37 (2010) 930–941.
- [16] B.T. Kim, G.L. Yoon, Laboratory modeling of laterally loaded pile groups in sand, *KSCE J. Civ. Eng.* 15 (2011) 65–75.
- [17] Deutschen Gesellschaft für Geotechnik e.V. (DGGT), *Empfehlungen des Arbeitskreises, Pfähle EA-Pfähle*, 2nd ed. Berlin : Wilhelm Ernst & Sohn; 2012.
- [18] D.A. Brown, C. Morrison, L.C. Reese, Lateral load behavior of pile group in sand, *J. Geotech. Eng.-ASCE* 114 (1998) 1261–1276.
- [19] N. Alati, V. Nava, G. Failla, F. Arena, A. Santini, On the fatigue behavior of support structures for offshore wind turbines, *Wind Struct.* 18 (2014) 117–134.
- [20] P. Passon, K. Branner, Load calculation methods for offshore wind turbine foundations, *Ships Offshore Struct.* 9 (2014) 433–449.
- [21] *Plaxis 3D user's manual* edited by Brinkgreve RBJ, Engin E, Swolfs WM. Delft, Plaxis bv; 2013.
- [22] Benz T. Small strain stiffness of soils and its numerical consequences Ph.D. Thesis. Stuttgart : Mitteilung 55 des Instituts für Geotechnik der Universität Stuttgart; 2007.
- [23] B.S. Knudsen, M.U. Østergaard, L. Ibsen, J.C. Clausen, Determination of p-y curves for bucket foundations in sand using finite element modeling, in: DCE Technical Memorandum; No.31, Alborg University Department of Civil Engineering, Alborg, 2013.
- [24] L. Bekken, Lateral behavior of large diameter offshore monopile foundations for wind turbines, in: M.Sc. Thesis, Delft University of Technology, Delft, 2009.
- [25] L.C. Reese, W.R. Cox, F.D. Koop, Analysis of laterally loaded piles in sand, in: *Proceedings of the Offshore Technology Conference*, Texas, 1974, pp. 95–105 (Paper No. OTC 2080).
- [26] M.R. Arta, The behavior of laterally loaded two-pile groups, in: Ph.D. Thesis, University of Durham, Durham, 1992.
- [27] L.C. Reese, W.F. Van Impe, *Single Piles and Pile Groups Under Lateral Loading*, 2nd ed., Taylor & Francis/Balkema, Leiden, 2011.
- [28] I. Manoliu, D.V. Dimitriu, N. Radulescu, G.H. Dobrecu, Load-deformation characteristics of drilled piers, in: *Proceedings of 11th International Conference on Soil Mechanics and Foundation Engineering*, San Francisco, 1985, pp. 1553–1558.
- [29] L.B. Ibsen, H.R. Roesen, T.K. Wolf, M. Hansen, K.L. Rasmussen, Assessment of p-y curves from numerical methods for a non-slender monopile in cohesionless soil, in: *Proceedings of the Twenty-third International Offshore and Polar Engineering Conference*, Alaska : International Society of Offshore and Polar Engineers (ISOPE), 2013, pp. 436–443.



این مقاله، از سری مقالات ترجمه شده رایگان سایت ترجمه فا میباشد که با فرمت PDF در اختیار شما عزیزان قرار گرفته است. در صورت تمایل میتوانید با کلیک بر روی دکمه های زیر از سایر مقالات نیز استفاده نمایید:

لیست مقالات ترجمه شده ✓

لیست مقالات ترجمه شده رایگان ✓

لیست جدیدترین مقالات انگلیسی ISI ✓

سایت ترجمه فا ؛ مرجع جدیدترین مقالات ترجمه شده از نشریات معتبر خارجی